ELSEVIER

Materials Science and Engineering A210 (1996) 64–75

MATERIALS SCIENCE & ENGINEERING A

Kinetics of directed oxidation of Al–Mg alloys in the initial and final stages of synthesis of Al_2O_3/Al composites

H. Venugopalan, K. Tankala, T. DebRoy*

Department of Materials Science and Engineering, Pennsylvania State University, University Park, PA 16802, USA

Received 29 March 1995; in revised form 6 July 1995

Abstract

In the directed oxidation of Al–Mg alloys, MgO forms in the initial stage. The mechanism of formation of MgO from the Al–Mg alloy in the initial stage of oxidation was studied. The variables studied were the total pressure in the reaction chamber and partial pressure of oxygen. The oxidation rate in the initial stage was proportional to both the oxygen partial pressure and oxygen diffusivity. These results suggest that MgO forms by reaction-enhanced vaporization of Mg from the alloy followed by oxidation of the Mg vapour in the gas phase. The end of the initial stage corresponds to the arrival of the oxygen front close to the melt surface, when spinel formation occurs.

The kinetics of formation of Al_2O_3 in the growth stage of directed oxidation of the Al–5wt.% Mg alloy was also investigated as a function of time, temperature and oxygen partial pressure. The growth rate decreased as a function of time, was practically independent of oxygen pressure and exhibited an activation energy of 361 kJ mol^{-1}. In the growth stage, the kinetics of oxidation is controlled by the rate of transport of oxygen through the alloy layer near the surface to the alumina–alloy interface.

Keywords: Directed oxidation; Al–Mg alloys; Composites

1. Introduction

The directed oxidation of molten aluminum alloys by vapor phase oxidants can be used to produce ceramic matrix composites. Under appropriate conditions of alloy composition, temperature and oxygen pressure, a rapid reaction of the molten alloy with the oxidant to form α-alumina occurs and the reaction product grows outward from the original metal surface [1]. The reaction is sustained by the wicking of liquid metal along interconnected microscopic channels in the alumina [1]. The resulting material is an Al_2O_3/Al composite with a three-dimensional network of metal channels [2]. Reinforced composites with the desired structural properties can be obtained by growing this "composite matrix" into preforms consisting of reinforcing particulates, whiskers or fibers of Al_2O_3, SiC, etc. [3–5]. Growth of the "composite matrix" into a preform typically involves no change in dimensions and hence problems associated with densification shrinkage in traditional ceramic processing are avoided [6]. Composites made by directed oxidation can be tailored to have good toughness, thermal shock resistance, wear resistance, high stiffness and high temperature stability. These composites are currently being used or evaluated for use in turbine engine components, armor applications, heat exchangers and furnace components [6].

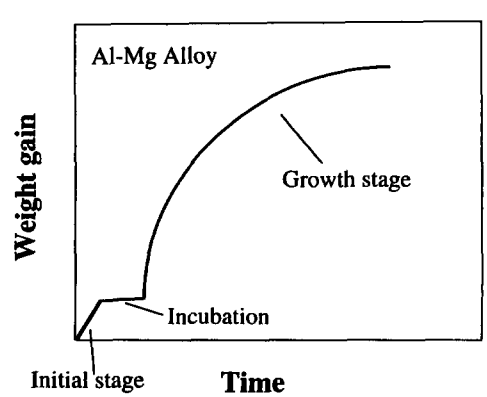

Fig. 1. Schematic plot of weight gain as a function of time for directed oxidation of Al–Mg alloys.

* Corresponding author.

SSDI 0921-5093(95)10072-5

The presence of dopants such as Mg, Zn or Si are crucial for directed oxidation to take place [1,7]. These dopants can be either applied to the surface of the aluminum exposed to the oxidant or, if soluble, alloyed with the parent metal. Three distinct stages can be observed in the oxidation of Al–Mg alloys at a given temperature [8] (Fig. 1). When the alloys are heated in argon to a given temperature and then exposed to an oxygen atmosphere, an initial stage of rapid weight gain occurs. During this period, MgO, formed by vapor phase oxidation, falls back on the crucible. The weight gain results from the formation of MgO [8]. Formation of a dense, thin layer of $MgAl_2O_4$ beneath the MgO halts the initial stage of oxidation and corresponds to the start of incubation [8]. The weight gain during incubation is small and corresponds to the thickening of the spinel layer [9]. During incubation, metal channels are observed to form in the spinel and the arrival of these metal channels at the top of the spinel is believed to correspond to the end of incubation and the start of the growth stage [8]. During growth, bulk oxidation of Al to Al_2O_3 occurs epitaxially on the spinel [9]. The amount of aluminum converted to alumina in the growth stage and the onset of the growth stage are critically dependent on the Mg composition in the alloy [1,8]. Since the residual Mg content in the alloy at the start of the growth stage is controlled by the amount of MgO that forms in the initial stage, the mechanism of the initial stage is clearly important. Although the amount of MgO at the surface of the melt plays an important role in the bulk oxidation of Al–Mg alloys, a review of the literature on directed oxidation of aluminum alloys reveals that the mechanism of initial stage oxidation is not completely understood.

Several models have been proposed to explain the kinetics of oxidation of Al to Al_2O_3 in the growth stage. It has been suggested that during the growth stage of directed oxidation of Al–Mg alloys a continuous MgO film exists at the top of the alumina matrix, with a thin aluminum alloy film separating the two layers [9,10] (Fig. 2). The presence of this continuous MgO film restricts the formation of a protective alumina layer on the surface. At the MgO–Al alloy film interface, MgO dissociates and oxygen dissolves in the Al alloy film. The magnesium ions formed by dissociation of MgO diffuse through the MgO layer to the MgO–air interface, where they are oxidized to regenerate MgO. During the outward transport of magnesium ions through MgO, electrical neutrality is maintained by the parallel transport of electronic defects. The oxygen dissolved in the alloy film in contact with the MgO layer is transported to the alloy film–alumina interface, where composite growth takes place epitaxially. The supply of aluminum to the alloy film–alumina interface is thought to be sustained by the wicking of metal through channels in the alumina. One or more

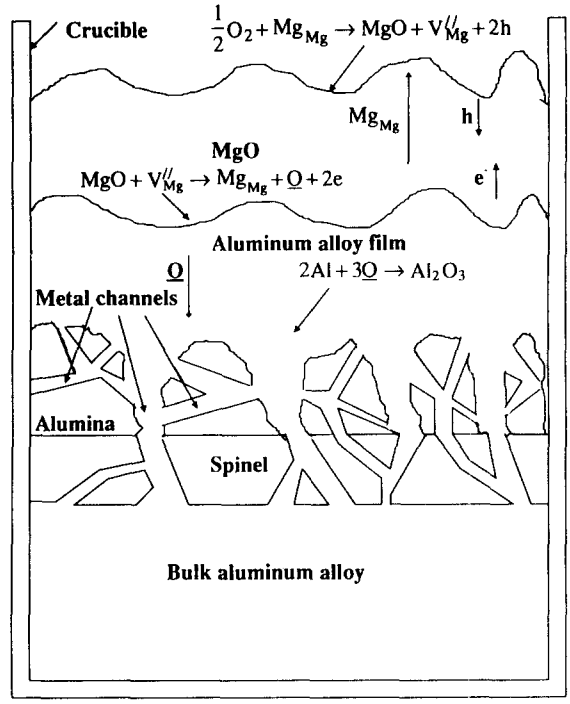

Fig. 2. Schematic diagram of the composite structure.

of the above-mentioned reaction steps could be the rate-controlling mechanism in the growth stage.

According to Nagelberg et al. [11], the rate of oxidation of Al–Mg–Si alloys in the growth stage is controlled by the electronic conductivity of the continuous external MgO layer. The rate was proportional to $P_{O_2}^{1/4}$, where P_{O_2} is the partial pressure of oxygen. According to this model [11], the oxidation kinetics in the growth stage is expected to be linear with an activation energy of 310 kJ mol^{-1}. To investigate the role played by electronic transport in the oxidation kinetics in the growth stage, DebRoy et al. [12] carried out directed oxidation experiments in which platinum wires were positioned inside the alloy so that the wires would extend through the composite matrix to the MgO layer at the top surface and facilitate electronic transport. They observed that the rate of oxidation in the growth stage was independent of the presence or absence of Pt wires, indicating that transport of electronic species does not control the kinetics of oxidation in the growth stage. Thus the lack of dependence of growth rate on electronic transport indicates that the model of Nagelberg et al. [11] is not necessarily applicable in predicting the growth kinetics of binary Al–Mg alloys [12].

Most previous studies of directed oxidation have investigated Al–Mg–Si alloys [7–11,13], since the presence of Si was considered necessary for the directed oxidation to occur. During oxidation of Al–Mg–Si alloys, Si is rejected into the near-surface alloy layer, since very little of it is incorporated into the alumina formed [14]. The increase in silicon concentration can

slow down the reaction kinetics unless back diffusion of silicon down the metal channels into the bulk alloy takes place rapidly. The transport of silicon within the metal channels adds significant complexity in the analysis of oxidation rates. Recently it has been shown that the directed oxidation of Al–Mg alloys can be initiated in the absence of silicon [12,15]. In this paper, to avoid complications in the interpretation of the reaction kinetics, we concentrate solely on the directed oxidation of binary Al–Mg alloys. The oxidation kinetics is studied by thermogravimetry. The variables investigated are the oxygen partial pressure, temperature and total pressure in the system. In order to understand the role of magnesium evaporation in the initial oxidation behavior of the alloy, the diffusion coefficient of magnesium vapor is varied by changing the total pressure. It is shown that formation of MgO in the initial stage occurs by gas phase oxidation of Mg vapor and that the MgO subsequently falls back on the alloy surface. The weight gain in the growth stage is monitored as a function of oxygen pressure and temperature. It is observed from the data that oxygen transport in the near-surface alloy layer controls the rate of formation of alumina in the growth stage of directed oxidation of binary Al–Mg alloys.

2. Experimental procedure

The thermogravimetric set-up used for studying the reaction kinetics in the directed oxidation of Al–Mg alloys consisted of a Cahn model 1000 automatic recording electric balance, a high temperature silicon carbide tube furnace and a gas flow and pressure control system. A schematic diagram of the experimental set-up is shown in Fig. 3. The balance had a sensitivity of 0.5 μg and the measurement accuracy was 0.1% of the range. The quartz reaction tube was of 48 mm internal diameter and had a 25 mm equitemperature zone at the center of the furnace. The furnace was equipped with an electronic temperature controller which regulated the temperature to ± 5 K.

A cylindrical sample, 14 mm in diameter and 8 mm in length, of an Al 5056 alloy (5 wt.% Mg, 0.10 wt.% Cu, 0.40 wt.% Fe, 0.10 wt.% Zn, 0.10 wt.% Mn and balance Al) was placed in an alumina crucible, 14.2 mm in diameter and 27 mm in length. The crucible containing the alloy was suspended by a platinum wire from the balance and positioned within the equitemperature zone of the furnace. Prior to conducting each experiment, the reaction tube was evacuated and purged with argon. The samples were then heated to the test temperature at a heating rate of 0.33 K s^{-1} in a pure argon atmosphere. When the target temperature was reached, a mixture of ultra-high purity oxygen and inert gas, argon, was introduced and the flow rates of oxygen and inert gas were controlled with the help of mass flow controllers to obtain a predetermined gas composition. Oxidation experiments were conducted at various partial pressures of oxygen, total pressures and reactor temperatures. Experiments conducted to examine the kinetics of oxidation in the composite growth stage were done at a constant total pressure of 93.3 kPa. The total gas flow rates in the initial stage and growth stage experiments were kept constant at 3333 mm^3 s^{-1} STP (298 K and 101.3 kPa) and 8333 mm^3 s^{-1} STP (298 K and 101.3 kPa) respectively. Higher total flow rates were used in the growth stage experiments so that the effect of widely differing oxygen pressures on the growth rate could be studied. Sample weight was continuously recorded using a computer data acquisition system. Subsequently, the recorded data were differentiated numerically to obtain the weight gain rate. The nominal cross-sectional area of the crucible, 154 mm^2, was used for the calculation of reaction rates.

In the experiments conducted to study the growth stage kinetics, the oxygen pressure in the initial stage was kept contant to ensure that the Mg composition in the bulk alloy at the start of the growth stage was kept constant. The effect of oxygen pressure on the growth rate was studied by subsequently changing the oxygen pressure in the growth stage. In this stage, in many cases, the oxidation product, Al_2O_3, grew along the crucible walls. The behavior is similar to the preferential growth of alumina on the crucible wall observed by Xiao and Derby [16] and Manor et al.[17]. The creeping is not surprising, since the MgO which forms in the gas phase coats the crucible walls. MgO is unstable in the presence of the Al–5wt.% alloy at 1373 K [18–20] and

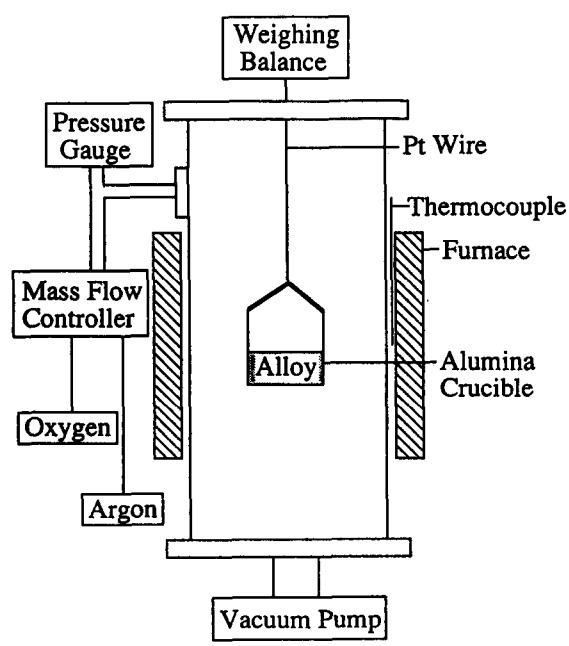

Fig. 3. Schematic diagram of the experimental set-up.

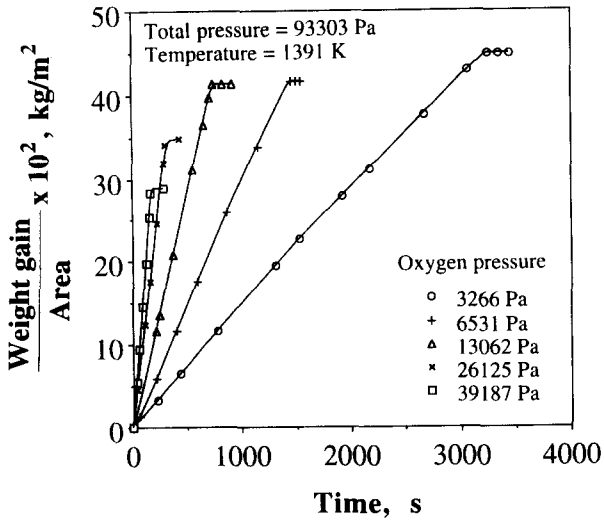

Fig. 4. Plot of weight gain per unit area vs. time for various oxygen pressures. The total pressure, temperature and total gas flow rate were maintained constant at 93 303 Pa, 1391 K, and 3333 mm s^{-1} STP respectively.

hence there is a net driving force for the reaction between Al and MgO. This causes Al to wet MgO [21], creep along the walls and react with oxygen in the external atmosphere to form alumina. The metal creeping leads to a change in the melt cross-sectional area exposed to the oxygen atmosphere with time and complicates the study of the reaction kinetics Fig. 4 reveals that the higher the oxygen pressure, the lower is the amount of MgO formed in the initial stage. Hence, to minimize creeping, the oxygen pressure was kept at a high value of 85.1 kPa in the initial stage and in the incubation period and subsequently reduced in the growth stage.

3. Results and discussion

A typical weight gain vs. time curve observed in the directed oxidation of Al–Mg alloys is shown in Fig. 1. The process starts with a rapid but limited oxidation event upon introduction of oxygen. The initial oxidation, corresponding to the formation of MgO, ends abruptly with the formation of an $MgAl_2O_4$ film on the alloy surface and is followed by an incubation period where the weight gain is small. The onset of bulk growth is marked by a substantial increase in the oxidation rate. The kinetics and mechanism of the initial and growth stages of composite synthesis are discussed in the following subsections.

3.1. Initial stage

Fig. 4 shows the weight gain per unit area of the Al–Mg alloy samples as a function of time in the initial stage of oxidation for various oxygen partial pressures at a temperature of 1391 K and total pressure of 93 303 Pa. It is observed that both the total weight gain during the initial stage of oxidation and the duration of the initial stage decreases with increasing partial pressure of oxygen. Furthermore, the rate of oxidation increases with increasing oxygen pressure. Several interesting questions arise from a perusal of these data. What is the mechanism of the initial stage of oxidation of the Al–Mg alloy? Why is the duration of the initial stage short at high oxygen pressures?

The oxidation experiments were terminated at the end of the initial stage and the samples were examined. Loose MgO powder was observed at the surface of the sample and on the inner walls of the crucible. The presence of MgO on the walls of the crucible indicates that the mechanism of oxidation in the initial stage involves evaporation of magnesium from the melt followed by its oxidation in the vapor phase. As Mg evaporates, a counterdiffusion of Mg vapor and O_2 gas in argon takes place. At a short distance from the surface of the alloy, Mg vapor reacts with oxygen to form an MgO mist according to the reaction

$$2Mg(v) + O_2 = 2MgO \quad (1)$$

As shown in Fig. 5, the gas phase is divided into two distinct zones, a magnesium vapor–argon region close to the melt surface and an oxygen–argon region above this region. At any given instant the molar fluxes of magnesium vapor, J_{Mg}, and oxygen, J_{O_2}, are given by

$$J_{Mg} = \frac{D_{Mg}(p_{MG} - p^{i}_{MG})}{\delta RT} \quad (2)$$

$$J_{O_2} = \frac{D_{O_2}(p_{O_2} - p^{i}_{O_2})}{(\Delta - \delta)RT} \quad (3)$$

where D_{Mg} is the interdiffusivity of the Mg(g)–Ar pair, D_{O_2} is the interdiffusivity of the Ar–O_2 pair, δ is the distance between the alloy surface and the location in the vapor phase where MgO forms, Δ is the sum of the thicknesses of the Mg and O_2 boundary layers, T is the temperature, p_{Mg} is the vapor pressure of Mg at the

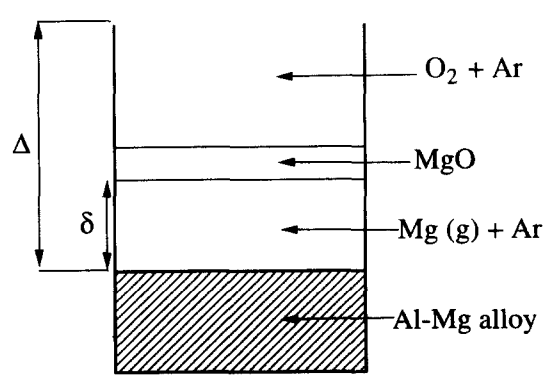

Fig. 5. Schematic diagram showing the magnesium and oxygen boundary layers formed in the gas phase above the melt and within the crucible during the initial stage of oxidation of Al–Mg alloys.

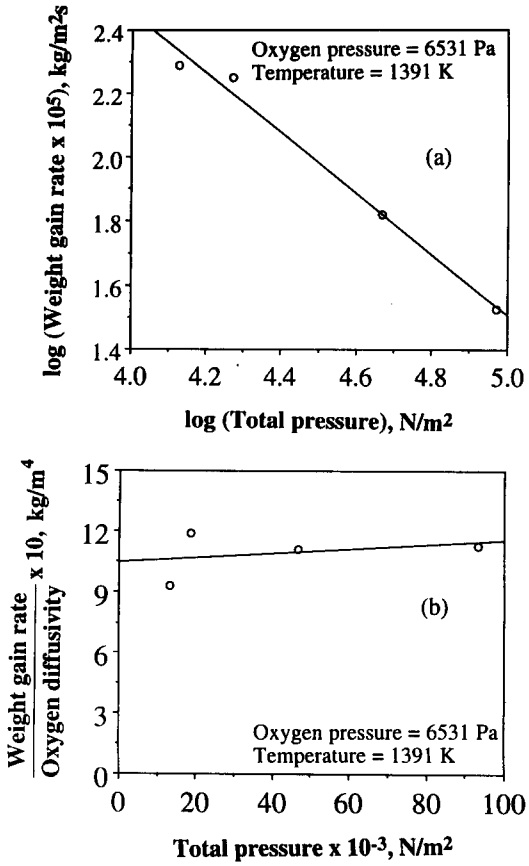

Fig. 6. (a) Weight gain rate in the initial stage of oxidation for different total pressures. (b) Ratio of weight gain rate in the initial stage to oxygen diffusivity in the reactive atmosphere for different total pressures. The oxygen pressure, temperature and the total gas flow rate were maintained constant at 6531 Pa, 1391 K, and 3333 mm s^{-1} STP respectively.

surface of the alloy, p^{i}_{Mg} and $p^{i}_{O_2}$ are the partial pressures of magnesium and oxygen at the reaction interface respectively and p_{O_2} is the partial pressure of oxygen at a distance Δ from the surface of the alloy. Since p^{i}_{Mg} and $p^{i}_{O_2}$ are much smaller than p_{Mg} and p_{O_2}, respectively, they can be neglected in Eqs. (2) and (3). From the stoichiometry of reaction (1) we obtain

$$J_{Mg} = 2J_{O_2} = \frac{2D_{O_2}p_{O_2}}{(\Delta - \delta)RT} = \frac{2D_{O_2}p_{O_2}}{RT\Delta}\left[1 + \frac{D_{Mg}p_{Mg}}{2D_{O_2}p_{O_2}}\right] \quad (4)$$

Furthermore, since $D_{Mg} \approx D_{O_2}$, the weight gain rate per unit area, R, is given by

$$R = 0.5M_{O_2}J_{Mg} = \frac{M_{O_2}D_{O_2}p_{O_2}}{RT\Delta}\left[1 + \frac{p_{Mg}}{2p_{O_2}}\right] \quad (5)$$

Eq. (5) explains the dependence of the weight gain rate in the initial stage on various variables such as oxygen pressure and diffusivity of oxygen in the gas phase. If the vaporization of magnesium is diffusion limited, a change in diffusion coefficient would result in a corresponding change in the weight gain rate. To confirm the proposed model, experiments were conducted at various total pressures for a constant oxygen partial pressure of 6531 Pa at 1391 K. Fig. 6(a) shows the variation in the observed weight gain rate with total pressure. The results show that the weight gain rate increases with decreasing total pressure. Since the binary diffusivity of gases is inversely proportional to the total pressure, a decrease in the total pressure results in an increase in the diffusivities of O_2 and Mg(g) in argon and should result in an increase in the weight gain rate. Fig. 6(b) is a plot of weight gain rate/oxygen diffusivity vs. total pressure. It is observed that weight gain rate/diffusivity is essentially constant as a function of the total pressure which is consistent with the predictions of Eq. (5). Thus the results confirm diffusion-limited vaporization of magnesium during the initial stage of oxidation of Al–Mg alloys.

Fig. 4 shows that the culmination of the initial stage of composite growth and the start of the incubation period is characterized by a sharp decrease in the weight gain rate. According to Vlach et al. [8], this sharp decrease in the rate occurs owing to the formation of a dense spinel layer which prevents magnesium vaporization and its subsequent oxidation. For alloy compositions between 0.19 and 12.0 mol% Mg, the magnesium aluminate spinel is thermodynamically more stable than MgO at 1400 K [18–20]. The spinel layer can form at the melt surface by one of the following reactions:

$$4MgO + 2Al(l) = MgAl_2O_4 + 3Mg(l) \quad (6)$$

$$Mg(l) + 2Al(l) + 2O_2 = MgAl_2O_4 \quad (7)$$

Formation of spinel by reaction (6) involves reaction of MgO with the alloy. If spinel formation occurs by way of reaction (6), the end of the initial stage would correspond to a critical amount of MgO required to form a spinel layer of certain thickness which would be impervious and stop further Mg vaporization. This entails that the same amount of MgO form at the end of the initial stage, irrespective of the experimental conditions of oxygen pressure and total pressure. However, it is observed from Figs. 4 and 6(a) that the weight gain at the end of the initial stage, which is a measure of the amount of MgO formed, is different for different oxygen pressures and total pressures. Thus the experimental data cannot be explained on the basis of spinel formation by reaction (6). Instead, the results are consistent with spinel formation in the presence of oxygen at the melt surface (reaction (7)).

At the start of the initial stage of oxidation, Mg vaporizing from the alloy surface reacts with the oxygen and hence spinel formation by reaction (7) cannot occur. However, the Mg vapor pressure over the melt decreases with the decrease in the Mg concentration in the melt. In effect, the oxygen front continuously moves

closer to the alloy melt surface (i.e. the Mg boundary layer thickness (δ) decreases) as the initial stage progresses. Numerical computation of concentration fields in the gas phase [22] indicates that for the highest oxygen pressure of 39 187 Pa (constant J_{Mg}), δ decreases by 45% while the Mg composition in the alloy changes similarly by 45%. This can be rationalized based on Eq. (2), which indicates that the change in δ would be proportional to the change in the Mg vapor pressure (or Mg composition in the alloy) if J_{Mg}, the vaporization rate, is constant. However, for the lower oxygen pressure of 3266 Pa, J_{Mg} decreases with time. Therefore the change in δ would no longer be proportional to the change in the Mg vapor pressure (Eq. (2)). Indeed, for the oxygen pressure of 3266 Pa, δ changes by 80% from 12 to 2 mm while the Mg composition in the alloy changes by 60%. It is found that at the end of the initial stage the value of δ is similar for the lowest and highest oxygen pressures [22]. The completion of the initial stage therefore corresponds to the time required for δ to become sufficiently small so that oxygen can reach the melt surface and react with the alloy to form spinel.

3.2. Growth stage

Fig. 7 is a plot of weight gain vs. time for an oxygen pressure of 85.1 kPa in the initial and incubation stages and varying oxygen pressures in the growth stage. It is

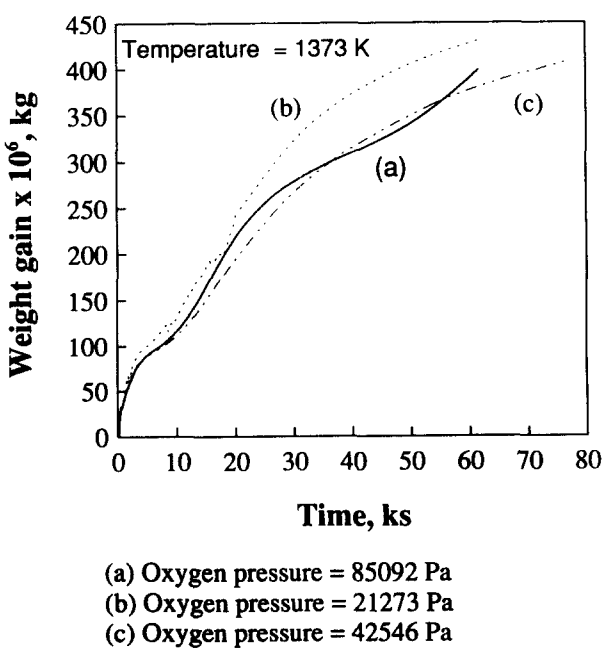

Fig. 7. Weight gain vs. time for different oxygen pressures in the growth stage: (a) 85 092, (b) 21 273 and (c) 42 546 Pa. The oxygen pressure was initially matained at 85 092 Pa for 7.2 ks and subsequently changed in the growth stage. The total pressure, temperature and total gas flow rate were maintained constant at 93 303 Pa, 1400 K, and 8333 $mm^3\ s^{-1}$ STP respectively.

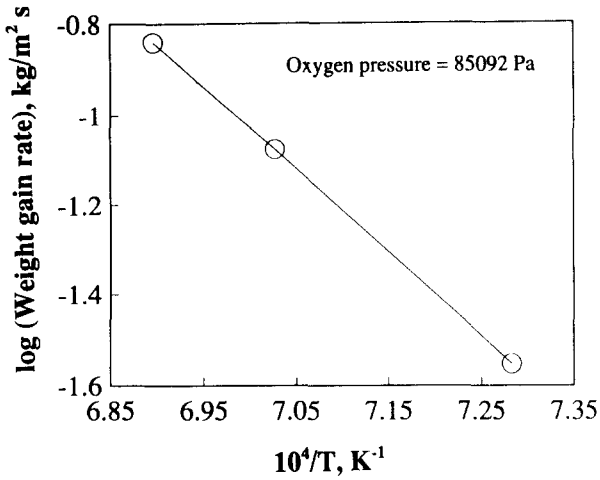

Fig. 8. Weight gain rate vs. temperature for an oxygen pressure of 85 092 Pa. The total pressure and total gas flow rate were maintained constant at 93 303 Pa and 8333 $mm^3\ s^{-1}$ STP respectively.

observed that the oxidation rate in the growth stage decreases with time and, within experimental uncertainty, remains independent of oxygen pressure. Weight gain, as a function of time, was also measured at various temperatures (1373–1450 K) for an oxygen pressure of 85.1 kPa. The weight gain rates are plotted as a function of temperature in Fig. 8 and the activation energy is found to be 361 kJ mol^{-1}. Several important questions arise from the perusal of the rate data. Why does the weight gain rate decrease with time? Why is the weight gain rate practically independent of oxygen pressure? What is the rate-controlling mechanism in the growth stage of directed oxidation of Al–Mg alloys?

Mechanism of composite growth. As shown in Fig. 2, the composite structure near the growth surface [11] consists of a continuous Al_2O_3-doped MgO layer on top of the alumina matrix, with a thin aluminum alloy film separating the two layers. At the MgO–Al alloy film interface, MgO dissociates and the oxygen dissolves in the alloy film and is transported to the Al_2O_3–alloy film interface, where the composite growth takes place epitaxially. The magnesium ions formed by the dissocation of MgO diffuse through the MgO layer to the MgO–air interface, where they are oxidized to regenerate MgO. The supply of liquid aluminum to the alloy film–alumina interface is sustained by wicking of metal through channels in the alumina. Thus the three possible rate-controlling steps in the growth of Al_2O_3/Al composites from Al–Mg alloys are (i) the flux of magnesium ions through the external MgO layer, (ii) the transport of liquid metal by capillarity through the interconnected metal channels in the alumina and (iii) dissociation of MgO and the subsequent flux of oxygen from the MgO–alloy film interface to the Al_2O_3–alloy film interface. The experimental results in Figs. 7 and 8 are analyzed below in detail to determine which of the

Table 1
Characteristics of various events in growth stage

Event	Oxygen pressure dependence of growth rate	Time dependence of growth rate	Activation energy (kJ mol^{-1})	Weight gain rate (mg cm^{-2} h^{-1})
Magnesium ion flux	$P_{O_2}^{1/4}$	Independent of time	310	17.44
Liquid metal transport	Independent of oxygen pressure	Decreases with time	6.1	6415
Oxygen transport through alloy film	Independent of oxygen pressure	Decreases with time	243.6	53.17
Experimental growth rate	Independent of oxygen pressure	Decreases with time	361	12.75

proposed steps are consistent with the observed growth rate and its dependence on time, oxygen pressure and temperature.

3.2.1. Transport of magnesium ions

Nagelberg et al. [11] developed a model for the transport of magnesium ions through the external MgO layer. Since MgO is unstable for the alloy compositions typically used in directed oxidation [18–20], MgO dissociates at the alloy film–MgO interface to give up oxygen which is subsequently transported to the alloy film–alumina interface. The MgO could be regenerated either by the outward diffusion of magnesium ions to the external surface or by the inward diffusion of oxygen ions to the MgO–alloy film interface (Fig. 2). According to Nagelberg et al. [11], the transport through the MgO layer is controlled by grain boundary diffusion of magnesium ions. This ionic transport is accompanied by electronic conduction (holes or electrons) to maintain charge neutrality and is taken to be the rate-limiting process. Near the external surface, in the Al_2O_3-doped MgO, the hole is the dominant electronic defect and its concentration is proportional to $P_{O_2}^{1/4}$, where P_{O_2} is the partial pressure of oxygen in the reaction chamber. This behavior follows from the following defect reactions for the dissolution of alumina and oxygen in MgO:

$$Al_2O_3 \rightarrow 2Al_{Mg}^{\bullet} + V_{Mg}'' + 3O_O \quad (8)$$

$$\tfrac{1}{2}O_2 \rightarrow O_o + V_{Mg}'' + 2h \quad (9)$$

Here V_{Mg}'' denotes a magnesium ion vacancy, $Al_{Mg}^{\bullet}$ represents the dissolved aluminum concentration in MgO and h indicates a hole. Similarly, for the low oxygen pressures near the metal surface the concentration of electrons in MgO would be high:

$$\tfrac{1}{2}O_2 + 2e^- \rightarrow O_o + V_{Mg''} \quad (10)$$

Thus the outward transport of magnesium ions in the MgO toward the external surface is accompanied by the transport of holes near the external surface and electrons near the metal layer to maintain electrical neutrality. Following the procedure of Nagelberg et al. [11], an expression can be derived for the flux of magnesium and the corresponding flux of oxygen at 1373 K. The oxygen flux J (gm cm^{-2} s^{-1}) is given as

$$J = 3.15 \times 10^6 P_{O_2}^{1/4} \exp\left(\frac{-310 \times 10^3}{RT}\right) \quad (11)$$

where P_{O_2} (atm) is the partial pressure of O_2, R (J mol^{-1} K^{-1}) is the gas constant and T (K) is the temperature. The activation energy for the process is 310 kJ mol^{-1}, which corresponds to the mobility of holes in MgO (Table 1).

Oxygen pressure and time dependences of magnesium ion transport. It is seen from Eq. (11) that if the magnesium ion flux through MgO is rate limiting, the oxygen flux (growth rate) would exhibit a $P_{O_2}^{1/4}$ dependence. Thus Eq. (11) predicts that for a change in oxygen pressure from 21.3 to 85.1 kPa the weight gain rate would increase by 41.4%. However, a 6.5% decrease in the weight gain rate is observed in the average experimental growth rate (Fig. 7) when the oxygen pressure is changed from 21.3 to 85.1 kPa. Eq. (11) also predicts that the oxygen flux should be independent of time. Experimentally, however, the weight gain rate (growth rate) decreases with time. Thus this mechanism cannot explain either the manner in which the rate varies with time or the growth rate dependence on oxygen pressure. Therefore this event is ruled out as a rate-limiting step.

3.2.2. Liquid metal transport

Rate expression. The reaction of Al with oxygen to form Al_2O_3 requires the continued supply of aluminum to the Al alloy film–Al_2O_3 interface. This is believed to occur via convective flow of metal by wicking through the thickening Al_2O_3 reaction product via the intercon-

nected metal channels. If the liquid metal transport through the metal channels is rate controlling, the total metal flow through the composite channels would determine the composite growth rate. Furthermore, the growth rate will show the same dependence on time and P_{O_2} as capillary flow. Therefore, the time and P_{O_2} dependence of metal flow rate and the corresponding oxygen weight gain rate need to be analyzed. As shown in Appendix A, the weight gain rate per unit area, J, is given by

$$J = \frac{48}{54}\frac{f\rho_{Al}}{4}\left(\frac{2R\gamma_{LV}\cos\theta}{\mu t}\right)^{1/2} \quad (12)$$

where f is the total metal channel area per unit area of the composite, ρ_{Al} is the density of molten aluminum alloy, R is the radius of the channel, γ_{LV} is the surface tension of the molten alloy, θ is the contact angle between the molten alloy and alumina, μ is the viscosity of the molten alloy and t is the time of oxidation.

Oxygen pressure and time dependences of rate of liquid metal transport. It is seen from Eq. (12) that if the liquid metal transport is rate controlling, the growth rate would be independent of oxygen pressure and decrease with time. The experimentally observed oxygen pressure and time dependences for liquid metal transport are qualitatively consistent with that predicted by Eq. (12). If the predicted growth rate is also in good agreement with the experimentally observed growth rate for the Al–5wt.%Mg alloy, the transport of liquid metal can be considered to be the rate-controlling step in the growth of Al_2O_3/Al composites.

Comparison of the rate of liquid metal transport with the experimental growth rate. The growth rate predicted by Eq. (12) is compared with the experimentally observed growth rates for Al–5wt.%Mg alloy at 1373 K and an oxygen pressure of 85.1 kPa (Fig. 7). The data used in the calculation are given in Table 2. For a weight gain of 300 mg, which corresponds to a composite thickness of 0.13 cm, the weight gain rate is predicted to be 6415 mg cm^{-2} h^{-1} based on equation (A8) in Appendix A, while the experimentally observed weight gain rate is found from Fig. 7 to be 10.8 mg cm^{-2} h^{-1}. It is seen that the experimentally observed weight gain rate is about two orders of magnitude lower than the lowest estimate of the predicted weight gain rate.

Table 2
Data used for calculation of rate of liquid metal transport

Property	Symbol	Value	Ref.
Total metal channel area per unit area of composite	f	10^{-5}	[2]
Density of aluminum (kg m^{-3})	ρ_{Al}	2300	[23]
Channel radius (m)	R	3×10^{-6}	[9]
Viscosity of molten aluminum (N s m^{-2})	μ	6.21×10^{-4}	[23]
Vapor pressure of magnesium (N m^{-2})	P_v	5019	[18–20]
Gravitational pressure (N m^{-2})	P_g	2955[a]	This study
Capillary pressure (N m^{-2})	P_c	6.3×10^5	Appendix A

[a]For a composite thickness of 0.00131 m. This corresponds to a weight gain of 3×10^{-4} kg.

The experimental results indicate that the weight gain rate decreases with time and is independent of the oxygen pressure. These trends are consistent with a situation where the transport of liquid metal controls the oxidation rate. However, the calculated weight gain rate is much higher than the experimentally observed value (Table 1). Furthermore, the theoretical activation energy for liquid metal transport corresponds to the temperature sensitivity of the viscosity of liquid aluminum alloy (Eq. (12)) and is about 6.1 kJ mol^{-1} [24], while the experimentally observed value is 361 kJ mol^{-1}. Thus the liquid metal transport through the metal channels does not control the rate of oxidation of Al to Al_2O_3 in the growth stage.

3.2.3. Oxygen transport through alloy film

Flux of oxygen. The flux of dissolved oxygen from the MgO–Al alloy interface to the Al_2O_3–Al alloy interface can be estimated using Fick's law as

$$J = \frac{16D_O(X_O^I - X_O^{II})}{LV_m} \quad (13)$$

where J denotes the flux of oxygen, D_O is the diffusion coefficient of oxygen in molten aluminum, X_O^I is the mole fraction of dissolved oxygen in the alloy film at the MgO–alloy film interface, X_O^{II} is the mole fraction of dissolved oxygen in the alloy film at the Al_2O_3–alloy film interface, L is the thickness of the alloy film and V_m is the molar volume of the alloy. The value of X_O^I can be estimated from the MgO–metal equilibrium

$$MgO = \underline{Mg} + \underline{O} \text{ (1 mol\%)} \quad (14)$$

where Mg and O denote magnesium and oxygen dissolved in the alloy film respectively. From reaction (14) we get

$$X_O^I = \frac{\exp(-\Delta G_M^\circ/RT)}{\gamma_{Mg}X_{Mg}} \quad (15)$$

where ΔG_M° is the standard free energy change of reaction (14), X_{Mg} is the mole fraction of magnesium in the aluminum alloy and γ_{Mg} is the activity coefficient for magnesium in liquid aluminum. A similar expression can be derived for X_O^{II} from the Al_2O_3–metal equilibrium

$$Al_2O_3 = 2Al(l) + 3\underline{O} \quad (16)$$

$$X_O^{II} = \frac{\exp(-\Delta G_A^\circ/3RT)}{(1 - X_{Mg})^{2/3}} \quad (17)$$

where ΔG_A° is the standard free energy change of reaction (16). It can be seen from Eqs. (15) and (17) that an increase in the Mg concentration leads to a decrease in the dissolved oxygen concentration at the MgO–alloy interface and an increase in the dissolved oxygen concentration at the Al_2O_3–alloy interface.

Oxygen pressure and time dependences of oxygen flux. From the standard free energies of formation of MgO, $MgAl_2O_4$ and Al_2O_3 [19,20] and the Al–Mg solution thermochemistry [18] it can be shown that Al_2O_3 is the stable phase in the Al–Mg–O system for alloys containing less than 0.19 mol% Mg at 1373 K. For alloy compositions from 0.19 to 12 mol% Mg in Al, $MgAl_2O_4$ is the stable phase, while MgO is the stable phase for an Mg concentration in the alloy film higher than 12 mol% Mg at 1373 K. The Al–Mg alloy in the composite channels is at equilibrium with $MgAl_2O_4$–Al_2O_3. Based on the available thermodynamic data [18–20], this equilibrium alloy composition is 0.19 mol% Mg at 1373 K. Several investigators [11,15,25] have measured the Mg concentration in the metal channels and shown that the composition remains at equilibrium with $MgAl_2O_4$–Al_2O_3 at the reaction temperature. The Al–Mg alloy wicks through the metal channels, reacts with the dissolved oxygen and forms fresh alumina epitaxially on the existing alumina. The epitaxial formation of fresh alumina is more likely to occur on the top surface of the existing alumina (alumina–alloy film interface) rather than on the walls of the channels (alumina + spinel–metal channel interface). This is because the oxygen transport through the alloy film is slow compared with the rate of transport of the alloy through the channels (Table 1). The solubility limit for Mg in Al_2O_3 is 0.012 mol% at 2073 K [26] and the solubility decreases rapidly with decreasing temperature. As the aluminum in the alloy gets oxidized to alumina, the concentration of magnesium in the alloy film tends to increase to values higher than 0.19 mol% Mg. The build-up of magnesium concentration in the alloy film continues with time unless magnesium back diffusion down the metal channels into the bulk alloy occurs at appreciable rates. Since the liquid metal transport through the channels to the reaction interface is fairly rapid, the solute enrichment is likely to continue. It can be seen from Eqs. (15) and (17) that when the magnesium concentration in the alloy increases, the equilibrium oxygen concentration at the MgO–alloy interface decreases. At the same time the dissolved oxygen concentration at the Al_2O_3–alloy interface increases. Thus the increase in magnesium concentration in the alloy film leads to a lower oxygen concentration gradient across the film. As a result, the rate of oxygen transport in the near-surface alloy layer decreases with time. Furthermore, it is observed from Eq. (13) that the rate is independent of oxygen pressure. These trends are consistent with the experimentally observed dependence of growth rate on time and oxygen pressure.

Table 3
Data used in calculation of oxygen transport through near-surface alloy layer

Property	Symbol	Value	Ref.
Diffusivity of oxygen in molten aluminum[a] ($m^2\ s^{-1}$)	D_o	1.3×10^{-8}	[24]
Thickness of alloy layer (m)	L	3×10^{-6}	[10]
Oxygen concentration in alloy film at MgO–film interface[b] (mol fraction)	X_O^I	2.5×10^{-5}	[18–20,28]
Oxygen concentration in alloy film at Al_2O_3–film interface[b] (mol fraction)	X_O^{II}	1.1×10^{-6}	[18–20,28]

[a]The tracer diffusivity of oxygen in molten aluminum is approximated by the diffusivity of aluminum in molten aluminum.
[b]Oxygen concentrations calculated at 1373 K for an Mg concentration of 0.19 mol% in the alloy film.

As the growth stage progresses, continued Mg enrichment in the near-surface alloy film can lead to the precipitation of $MgAl_2O_4$ spinel between the MgO and the underlying metal, as observed by several investigators [8,9,27]. $MgAl_2O_4$ forms beneath the MgO rather than on top of Al_2O_3 owing to nucleation considerations [27]. The spinel subsequently demixes owing to the presence of an oxygen gradient, exposing the alloy film to MgO, leading to fresh nucleation of Al_2O_3 on the existing alumina layer [9,27]. This is consistent with the proposed mechanism for the growth stage, where the oxygen required for alumina formation is supplied by dissociation of MgO. The observed continuing decrease in the growth rate with time [8] is consistent with our proposed model. Thus, notwithstanding the formation of the $MgAl_2O_4$ spinel, the proposed mechanism for the growth stage is expected to hold.

Oxygen flux through the near-surface alloy layer and the growth rate. The data used in Eq. (13) for the calculation of the maximum rate of oxygen transport are presented in Table 3. Note that the oxygen transport rate would be maximum at the start of the growth stage when the Mg concentration in the alloy film corresponds to about 0.19 mol%, i.e. the Mg concentration in the alloy corresponding to the $MgAl_2O_4/Al_2O_3$ equilibrium at 1373 K. The maximum rate of oxygen transport at 1373 K is estimated to be 53.17 mg cm^{-2} h^{-1}. This estimate is within an order of magnitude of the experimentally observed maximum growth rate of 12.75 mg cm^{-2} h^{-1}. The estimated rate for oxygen transport would be exactly equal to the experimental growth rate for a metal layer thickness of 12 μm. This value of thickness of the metal layer is higher than the values (1–3 μm) reported by Antolin et al. [10]. How-

ever, it is probably not unreasonable in view of the uncertainties involved in the calculation and the possibility that the metal layer thickness during the reaction may be higher than that observed after cooling to room temperature. The experimentally determined rate values are consistent with possibility that the oxygen transport through the metal layer is the rate-limiting step in the composite growth stage.

Activation energy for oxygen transport. Since the oxygen concentration at the MgO–alloy film interface is much higher than the dissolved oxygen concentration at the Al_2O_3–metal interface (Table 3), Eq. (13) can be approximated as

$$J = \frac{16 D_O X_O^l}{L V_m} \simeq \frac{16 D_O \exp(\Delta S_M^\circ / R) \exp(-\Delta H_M^\circ / RT)}{\gamma_{Mg} X_{Mg} L V_m} \quad (18)$$

where ΔH_M° is the standard enthalpy change for reaction (14) and ΔS_M° is the standard entropy change for reaction (14). The activation energy for diffusion in liquid aluminum is small (6.1 kJ mol^{-1}) [24] and hence very little variation is expected in the value of D_O over the narrow temperature range from 1373 to 1450 K examined in this study. The activation energy for oxygen transport is deduced from Eq. (18) as ΔH_M°, and is equal to 243.6 kJ mol^{-1} [18–20,28]. Thus the observed activation energy and weight gain rate in the growth stage are in fair agreement with those predicted for oxygen transport through the near-surface alloy layer. Considerations of the liquid metal transport through channels in the composite or the magnesium ion transport through the MgO layer cannot explain the observed oxidation behaviour. The predictions of the oxygen transport model are consistent with the observations of Vlach et al. [8] and Xiao and Derby [15], who reported parabolic oxidation kinetics in the growth stage and an activation energy of around 270 kJ mol^{-1}. The transport of oxygen through the near-surface alloy layer is the rate-controlling event in the growth stage of directed oxidation of binary Al–Mg alloys in the temperature range 1373–1450 K.

4. Summary and conclusions

The oxidation rates in the initial and growth stages of directed oxidation of Al–Mg alloys have been investigated. The effect of diffusivities of oxygen and magnesium on the initial weight gain rate was examined by varying the external pressure and maintaining the oxygen pressure in the argon–oxygen mixture constant. In the initial stage, MgO forms by vapor phase oxidation of Mg(g) and falls back in the crucible. The weight gain rate in the initial stage increases with increase in oxygen pressure and oxygen diffusivity. These results confirm the reaction-enhanced gaseous diffusion-limited vaporization of Mg in the initial stage of oxidation of Al–Mg alloys. It is suggested that the end of the initial stage corresponds to the time when the oxygen front essentially collapses on to the alloy surface.

The weight gain rate in the growth stage decreased with time and was independent of oxygen pressure. The activation energy for the growth process was found to be 361 kJ mol^{-1}. The growth of the Al_2O_3/Al composite comprises the following three processes: (i) the diffusion of magnesium ions through an external MgO layer, (ii) the dissolution and diffusion of oxygen in a near-surface layer of aluminum alloy and (iii) the transport of liquid metal through capillaries in the composite. The data indicate that the rate of oxygen transport through the near-surface molten alloy layer controls the rate of oxidaton of aluminum to alumina in the growth stage.

Acknowledgements

This work was supported by the National Science Foundation, Division of Materials Research under grant DMR-9118075. We thank Professor R. Roy for helpful discussions.

References

[1] M.S. Newkirk, A.W. Urquhart, H.R. Zwicker and E. Breval, Formation of Lanxide™ ceramic composite materials, *J. Mater. Res.*, *1*(1) (1986) 81–89.

[2] H. Venugopalan, K. Tankala and T. DebRoy, Electrical conductivity of alumina/aluminum composites synthesised by directed metal oxidation. *J. Am. Ceram. Soc.*, *77*(11) (1994) 3045–3047.

[3] M.S. Newkirk, H.D. Lesher, D.R. White, C.R. Kennedy, A.W. Urquhart and T.D. Claar, Ceramic matrix composites: matrix formation by the directed oxidation of molten metals. Ceram. Eng. Sci. Proc., *8*(7–8) (1987) 879.

[4] C.A. Andersson, P. Barron-Antolin, G.H. Schiroky and A.S. Fareed, Properties of fiber-reinforced Lanxide™ alumina matrix composites. in *Whisker and Fiber Toughened Ceramics*, ASM International, Materials Park, OH, 1988, pp. 209–215.

[5] A.S. Nagelberg, A.S. Fareed and D.J. Landini, Production of ceramic matrix composites for elevated temperature applcations using the DIMOX™ directed metal oxidation process, in *Processing and Fabrication of Advanced Materials*, Minerals, Metals and Materials Society, 1992, pp. 127–142.

[6] A.W. Urquhart, Novel reinforced ceramics and metals: a review of Lanxide's technologies, *Mater. Sci. Eng.*, *A144* (1991) 75–82.

[7] A.S. Nagelberg, Growth kinetics of Al_2O_3/metal composites from a complex aluminum alloy, *Solid State Ionics*, *32–33* (1989) 783–788.

[8] K.C. Vlach, O. Salas, H. Ni, V. Jayaram, C.G. Levi and R. Mehrabian, A thermogravimetric study of the oxidative growth of Al_2O_3/Al composites, *J. Mater. Res.*, *6*(9) (1991) 1982–1995.

[9] O. Salas, H. Ni, V. Jayaram, K.C. Vlach, C.G. Levi and R. Mehrabian, Nucleation and growth of Al_2O_3/metal composites by oxidation of aluminum alloys, *J. Mater. Res.*, *6*(9) (1991) 1965–1981.

[10] S. Antolin, A.S. Nagelberg and D.K. Creber, Formation of Al_2O_3/metal composites by the directed oxidation of molten aluminum–magnesium–silicon alloys: Part I, Microstructural development, *J. Am. Ceram. Soc.*, *75*(2) (1992) 447–545.
[11] A.S. Nagelberg, S. Antolin and A.W. Urquhart, Formation of Al_2O_3/metal composites by the directed oxidation of molten aluminum–magnesium–silicon alloys: Part II, Growth kinetics, *J. Am. Ceram. Soc.*, *75*(2) (1992) 455–462.
[12] T. DebRoy, A. Bandhopadhyay and R. Roy, Oxide matrix composite by directional oxidation of a commercial aluminum–magnesium alloy, *J. Am. Ceram. Soc.*, *77*(5) (1994) 1296–1300.
[13] A.S. Nagelberg, Observations on the role of Mg and Si in the directed oxidation of Al–Mg–Si Alloys, *J. Mater. Res.*, *7*(2) (1992) 265–668.
[14] M. Hillert, B. Sundman and X. Wang, A thermodynamic evaluation of the Al_2O_3–SiO_2 system, *Trita-Mac 402*, Royal Institute of Technology, Stockholm, 1989.
[15] P. Xiao and B. Derby, Alumina/aluminum composites formed by the directed oxidation of aluminum using magnesia as a surface dopant, *J. Am. Ceram. Soc.*, *77*(7) (1994) 1771–1776.
[16] P. Xiao and B. Derby, Alumina/aluminum composites formed by the directed oxidation of aluminum using sodium hydroxide as a surface dopant, *J. Am. Ceram. Soc.*, *77*(7) (1994) 1761–1770.
[17] E. Manor, H. Ni, C.G. Levi and R. Mehrabian, Microstructure evolution of SiC/Al_2O_3/Al-alloy composites produced by melt oxidation, *J. Am. Ceram. Soc.*, *76*(7) (1993) 1777–1787.
[18] B.L. Tiwari, Thermodynamic properties of liquid Al–Mg alloys measured by the emf method, *Metall. Trans. A*, *18* (1987) 1645–1651.
[19] M.W. Chase, Jr., C.A. Davies, J.R. Bowary Jr., D.J. Fromp, R.A. McDonald and A.N. Syverud, *JANAF Thermochemical Tables*, American Chemical Society, Washington, DC, 3rd edn., 1986.
[20] O. Kubaschewski, C.B. Alcock and P.J. Spencer, *Materials Thermochemistry*, Pergamon, New York, 1993.
[21] I. Aksay, C.E. Hoge and J.A. Pask, Wetting under chemical equilibrium and nonequilibrium conditions, *J. Phys. Chem.*, *78*(12) (1974) 1778–1783.
[22] H. Venugopalan, K. Tankala and T. DebRoy, Probing the initial stage of synthesis of Al_2O_3/Al composites by directed oxidation of Al–Mg alloys, *Metall. Mater. Trans.*, *27B* (1996) 43–50.
[23] E.A. Brandes and G.B. Brook (eds.), *General Physical Properties: Smithells Metals Reference Handbook*, Butterworth–Heinemann, London, 7th edn., 1992, p. 14–10.
[24] F.S. Levin, Polytherms of the viscosity and self-diffusion of molten aluminum, *Izv. Akad. Nauk SSSR, Met.*, *5* (1971) 72–78.
[25] M. Sindel, N.A. Travitsky and N. Claussen, Influence of magnesium–aluminum spinel on the directed oxidation of molten aluminum alloys, *J. Am. Ceram. Soc.*, *73*(9) (1990) 2615–2618.
[26] K. Ando and M. Momoda, Solubility of MgO in single crystal Al_2O_3, *J. Ceram. Soc. Jpn., Int. Edn.*, *95* (1987) 343-347.
[27] O. Salas, V. Jayaram, K.C. Vlach, C.G. Levi and R. Mehrabian, Banded microstructures in Al_2O_3/Al composites produced by oxidation of molten Al–Mg alloys, in V.A. Ravi and T.S. Srivatsan (eds.), *Processing and Fabrication of Advanced Materials for High Temperature Applications*, TMS, 1992.
[28] S. Otsuka and Z. Kozuka, Thermodynamic study of oxygen in liquid elements of group Ib to VIb, *Trans. Jpn. Inst. Met.*, *22*(8) (1981) 558–566.
[29] T. Young, *Trans. R. Soc.*, *95* (1805) 65.
[30] P. Nikopoulos, Surface, Grain-boundary and interfacial energies in Al_2O_3 and Al_2O_3–Sn, and Al_2O_3–Co Systems, *J. Mater. Sci.*, *20* (1985) 3993–4000.

Appendix A: Determination of rate expression for liquid metal transport

The volumetric flow rate of liquid alloy through metal channels in the alumina (capillaries) is given by the Poiseuille equation

$$\frac{dV}{dt} = \frac{\pi R^4 \Delta P}{8\mu x} \tag{A1}$$

where R is the capillary radius, ΔP is the pressure difference driving the flow, μ is the viscosity of the liquid alloy and x is the depth of penetration of the liquid at time t.

The pressure difference ΔP can be represented as

$$\Delta P = P_c - P_v - P_g \tag{A2}$$

where P_c is the capillary pressure, P_v is the vapor pressure of magnesium in the channel and P_g is the gravitational pressure due to the weight of the liquid in the channel. The capillary pressure P_c driving the flow is given by the expression

$$P_c = \frac{2\gamma_{LV}\cos\theta}{R} \tag{A3}$$

where γ_{LV} is the surface tension of the liquid aluminum alloy and θ is the contact angle between the liquid Al alloy and alumina. Exact values of the contact angle θ and the surface tension γ_{LV} are not available. However, they can be estimated as shown below.

From Young's equation [29] we have

$$\gamma_{LV}\cos\theta = \gamma_{SV} - \gamma_{SL} \tag{A4}$$

where γ_{SV} is the surface energy of alumina and γ_{SL} is the interfacial energy betwen the molten aluminum alloy and the solid Al_2O_3. Since the metal channels are present in the grain boundaries of alumina, the metal is considered to have spread along the grain boundaries [1]. The condition for metal spreading is given by the equation

$$\gamma_{SL} \leqslant \frac{\gamma_{SS}}{2} \tag{A5}$$

where γ_{SS} is the grain boundary energy in alumina. A lower estimate for $\gamma_{LV}\cos\theta$ is therefore given as

$$\gamma_{LV}\cos\theta = \gamma_{SV} - \frac{\gamma_{SS}}{2} \tag{A6}$$

From Eqs. (A4) and (A5) it can be seen that the higher estimate for $\gamma_{LV}\cos\theta$ can be determined by setting γ_{SL} as zero. The values of γ_{SV} and γ_{SS} can be estimated from the data of Nikolopoulos [30]. The lower and higher estimates for $\gamma_{LV}\cos\theta$ at 1373 K are 0.9455 and 1.4826 J m^{-2} respectively.

For the lower estimate of $\gamma_{LV}\cos\theta$, P_c is 9.884×10^5 N m^{-2} at 1373 K. From Table 3 it is seen that P_g and

P_v are much smaller than P_c and are therefore neglected in the determination of ΣP. Therefore the mass flow rate of Al, dM/dt (mol s^{-1}), through a single metal channel is given as

$$\frac{dM}{dt} = \rho_{Al}\frac{dV}{dt} = \frac{\rho_{Al}\pi R^3 \gamma_{LV}\cos\theta}{4\mu x} \quad \text{(A7)}$$

If f is the ratio of the total metal channel area to the area of the composite, the total mass flow rate of Al per unit area of the composite is $f\,dM/dt/\pi R^2$. Formation of alumina requires 48 g of oxygen for every 54 g of aluminum. Hence the oxygen weight gain rate per unit area, J, is given as

$$J = \frac{48}{54} f \frac{dM/dt}{\pi R^2} = \frac{48}{54}\frac{f\rho_{Al} R\gamma_{LV}\cos\theta}{4\mu x} \quad \text{(A8)}$$

Eq. (A1) can be rewritten as

$$\pi R^2 \frac{dx}{dt} = \frac{\pi R^4 \Delta P}{8\mu x} = \frac{\pi R^3 \gamma\cos\theta}{4\mu x} \quad \text{(A9)}$$

Integrating Eq. (A9), we get an expression for the depth of liquid penetration, x, as a function of time t:

$$x = \left(\frac{R\gamma_{LV}\cos\theta t}{2\mu}\right)^{1/2} \quad \text{(A10)}$$

Using the above expression for x in equation (A8), we get a relation between the flux J and the time of oxidation, t:

$$J = \frac{48}{54} f \frac{\rho_{Al}}{4}\left(\frac{2R\gamma_{LV}\cos\theta}{\mu t}\right)^{1/2} \quad \text{(A11)}$$